ADAPTIVE MESH REFINEMENT IN ELECTROMAGNETIC PROBLEMS

Alejandro Díaz-Morcillo[1], Luis Nuño[2], Juan V. Balbastre[2], David Sánchez-Hernández[1]

[1]*Universidad Politécnica de Cartagena, Cartagena, Murcia, Spain. alejandro.diaz@upct.es*
[2]*Universidad Politécnica de Valencia, Valencia, Spain. lnuno@dcom.upv.es*

ABSTRACT

This paper describes an adaptive mesh refinement algorithm for improving the accuracy in the solution of electromagnetic problems in transmission lines. A residual error indicator is used for detecting the refinement zones, and two *h*-refinement techniques for triangular meshes (the longest edge bisection and the regular split) are applied for increasing the degrees of freedom in the mesh. This procedure has been applied in several structures and the results show that the adaptive meshing allows obtaining accurate solution with a small amount of unknowns.

Keywords: adaptive meshing, mesh refinement, error indicator, triangles, electromagnetics

1. INTRODUCTION

Adaptive mesh refinement has been successfully used in civil engineering and fluid dynamics applications in last years. In this work, an adaptive finite element method for electromagnetic problems in transmission lines is presented.

This type of problems are governed by the vector wave equation:

$$\nabla \times \mu^{-1} \nabla \times \vec{u} - \omega^2 \vartheta \vec{u} \qquad (1)$$

where $\vec{u}$ is the electric or magnetic field (depending on the formulation used), μ and ϑ are magnetic and dielectric properties of the materials, and ω is the angular frequency of the problem.

The application of the finite element method (FEM) on this partial differential equation yields an eigensystem, whose eigenvalues are the propagation constants for the different solutions of the problem. If a direct eigensystem solver is used, the computational cost of the problem increases approximately as n^3, where n is the number of unknowns in the mesh. Adaptive methods try to distribute the degrees of freedom of the problem in such a way that an accurate solution can be obtained maintaining a low number of unknowns. In that sense, the adaptation procedure generates an optimal mesh, that is, the best mesh for a specific problem.

Figure 1 shows the flow diagram of a general adaptive procedure, where, at each iterative step, the problem is solved, an indication of the error for each element is obtained and the mesh is refined in those zones with a bigger error.

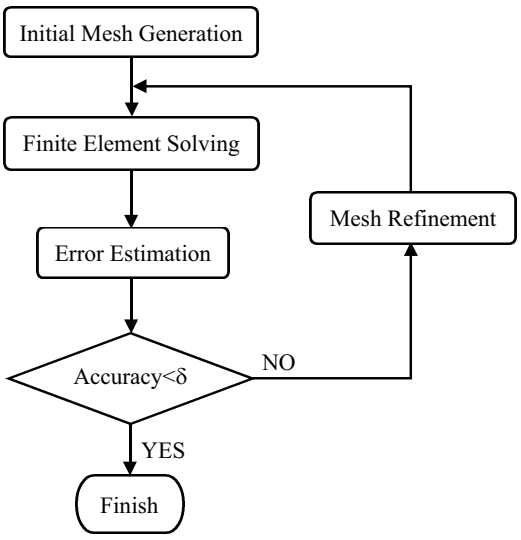

Figure 1. Adaptive mesh refinement flow diagram

For error detection, a residual error indicator [1] [2] has been used, although it is possible to employ other type of indicator, as patch recovery or smoothing indicators [3] [4] [5].

Basically, the residual error indicator measures the non-fulfillment of the vector wave equation and the boundary conditions:

$$\left\|\vec{e}^{\,i}\right\|^2 = f_s \frac{h_i^2}{\lambda_{\nu_i^{-1},min}\, p} \iint_{\Omega^e} \vec{r}_s^{\,i^*} \cdot \vec{r}_s^{\,i}\, d\Omega + f_l \frac{h_i}{\lambda_{\nu_i^{-1},min}\, p} \sum_{\Gamma_k \in \Gamma^i_{\text{int,Neu}}} \int_{\Gamma_k} \vec{r}_l^{\,k^*} \cdot \vec{r}_l^{\,k}\, d\Gamma \tag{2}$$

where the first term is the measure of the inner residual, and the second one measures the singular residual at the inner edges $\vec{r}_l^{\,k}\big|_{\text{int}}$ or Neumann boundary edges $\vec{r}_l^{\,k}\big|_{\text{Neumann}}$, f_s and f_l are weighting factors for both residuals, h_i is the size of the element (that is, the length of the longest edge in triangular elements), $\lambda_{\nu_i^{-1},min}$ is the smaller eigenvalue of the tensor ν_i^{-1}, and p is the degree of the interpolation functions employed in the FEM (in this work p=1).

The internal and singular residuals are:

$$\vec{r}_s^{\,i} = \nabla \times \nu_i^{-1} \nabla \times \vec{u}^{\,i} - \omega^2 \vartheta_i \vec{u}^{\,i} \tag{3}$$

$$\vec{r}_l^{\,k}\big|_{\text{int}} = \hat{n} \times \left(\nu_1^{-1} \nabla \times \vec{u}_1 - \nu_2^{-1} \nabla \times \vec{u}_2 \right) \tag{4}$$

$$\vec{r}_l^{\,k}\big|_{\text{Neumann}} = \hat{n} \times \nu_i^{-1} \nabla \times \vec{u}^{\,k} \tag{5}$$

where $\vec{u}^{\,e}$ is the solution of the FEM in the element i and $\vec{u}^{\,k}$ is that solution at the edge k.

This measure of the error is qualitative, that is, allows to detect elements or zones in the mesh with a bigger error, but it does not provide a bound of the error in the problem.

2. MESH REFINEMENT

2.1 Element Selection

The qualitative measure of the error, provided by the elemental indicator, allows selecting those elements with a bigger error. As a criterion, elements which fulfil

$$\left\|e^i\right\| > \kappa \|e\|_{max} \tag{6}$$

are selected for refinement.

In (6) $\left\|e^i\right\|$ is the error indication for the element i, $\|e\|_{max}$ is the maximum error in the mesh and κ $(0 < \kappa < 1)$ is a parameter which controls the number of elements to be refined and, therefore, the number of new elements at each step of the adaptive process. When κ is close to 1, the refinement takes place only at the elements with an error measure close to the maximum. This behavior implies a lot of steps in the adaptive process for obtaining accurate results. On the other hand, when κ is close to 0, a great quantity of elements are refined, even those with a little error. So, the computational cost of the FEM solver is highly increased and most of the new unknowns do not improve the accuracy of the solution. The results presented in this paper have been obtained with κ =0.5. Figure 2 shows a scheme of this refinement.

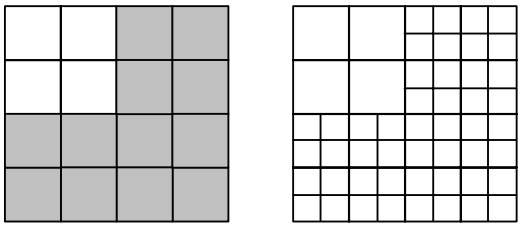

a) b)

Figure 2. Simple refinement: a) selected elements, b) refined mesh

Also, it is possible to design a multiple-level refinement [6] [7] [8] where the refinement criterion specifies several thresholds and several refinement intensities:

- $\left\|e^i\right\| \le \kappa_1 \|e\|_{max} \Rightarrow$ no refinement
- $\kappa_p \|e\|_{max} < \left\|e^i\right\| \le \kappa_{p+1} \|e\|_{max} \Rightarrow$ p refinement
- $\kappa_n \|e\|_{max} < \left\|e^i\right\| \Rightarrow$ maximum refinement

where $\kappa_p \in [0,1[$ and $\kappa_p < \kappa_{p+1}$.

This treatment will be studied in future work. The corresponding scheme (for 2-level refinement) is shown in figure 3.

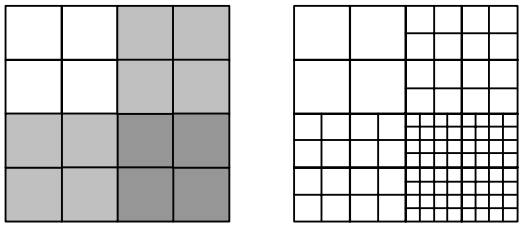

a) b)

Figure 3. Multiple refinement (2-level): a) selected elements, b) refined mesh

2.2 Element Split

In an *h*-refinement approach, there are different ways for refining the mesh. For instance, by adding new nodes in the selected elements and running a Delaunay triangulation [9]. In this work, procedures based on the "longest edge" bisection [10] and the regular split of triangles have been employed. The first technique splits the triangle up into two new elements (figure 4), and the second one into four elements with the same aspect ratio (figure 5a). Moreover, a maximum angle criterion (figure 5b) has been applied in order to obtain an additional improvement in the aspect ratio of some triangles. It is very important to maintain or improve the regularity of the elements throughout the adaptive procedure because the exactness of the FEM solution is directly related to it.

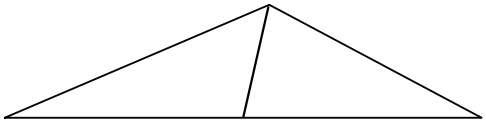

Figure 4. Longest edge (1:2) bisection

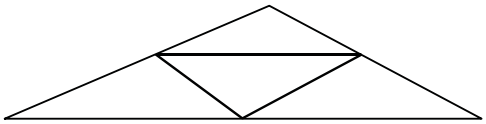

a)

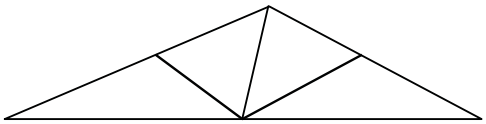

b)

Figure 5. Regular (1:4) split: a) normal, b) with maximum angle criterion

These two types of split lead to non-conformal meshes, as those of the figure 2 (quadrilaterals) or figure 6 (triangles). In order to obtain a conformal mesh, that is, to avoid "hanging nodes", a new generation of elements is needed (figure 7).

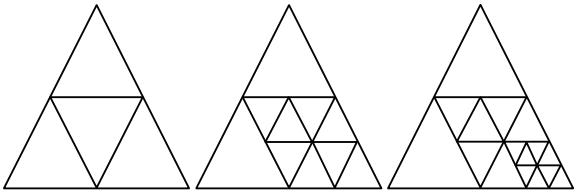

Figure 6. Non-conformal meshes: a) initial mesh, b) first refinement, c) second refinement

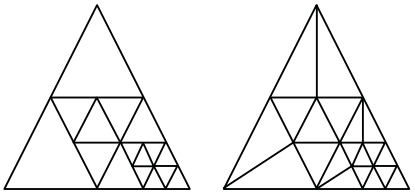

Figure 7. Generation of conformal mesh

In both split techniques, five non-conformal situations can be identified:

1. The element has hanging nodes in its three edges.
2. The element has hanging nodes in the two shortest edges.
3. The element has a hanging node in the longest edge.
4. The element has a hanging node in a different edge than the longest one.
5. The element has a hanging node in the longest edge and other one in other edge.

The corresponding solutions for these situations are (figure 8):

1. Regular split (1:4).
2. Regular split (1:4).
3. Union of the hanging node and the opposite vertex (1:2 split).
4. Union of the hanging node and the middle point of longest edge + union of the middle point of the longest edge and the opposite vertex.
5. Union of the hanging node and the middle point of longest edge + union of the middle point of the longest edge and the opposite vertex.

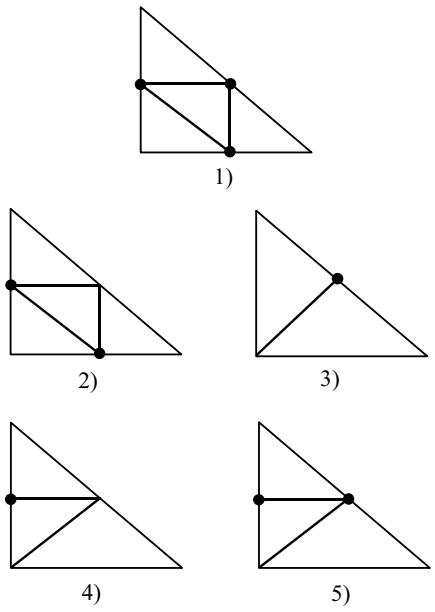

Figure 8. Solution of non-conformal cases

This strategy guarantees that in every mesh of the adaptation process the minimum angle is, at least, the half of the minimum angle in the initial mesh; that is, the loss of regularity in the elements is bounded.

3. RESULTS

The adaptive refinement procedure has been applied on several waveguiding structures. Here, the results obtained for structures with abrupt variation in the field distribution or singularities are shown. In those cases, an adaptive procedure improves significantly the accuracy of the FEM solution obtained from a uniform or graded meshes

3.1. L-shaped Homogeneous Waveguide

Figure 9 shows the transversal component (the dominant one) of the electric field distribution for the first mode or solution. A singularity in the electric field can be observed at the inner corner of the guide. Therefore, the optimal mesh must accumulate more degrees of freedom in that zone.

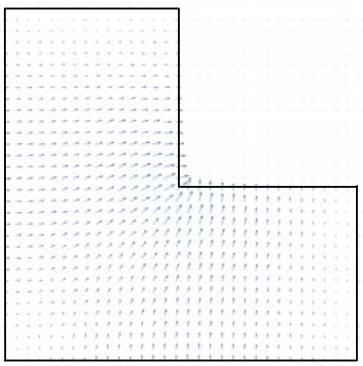

Figure 9. Transversal component of the first-mode electric field in an L-shaped homogeneous waveguide

The quality of the adaptive procedure can be established by comparing the convergence of the solution (the eigenvalue) with that obtained from the classical FEM. The convergence for this one has been obtained using different uniform meshes (figure 10) for the same problem, which have been generated, as the graded meshes for the other examples, by means on an hybrid advancing front / interpolation method [11] [12]. The first of these meshes is, also, the initial mesh for the adaptive process.

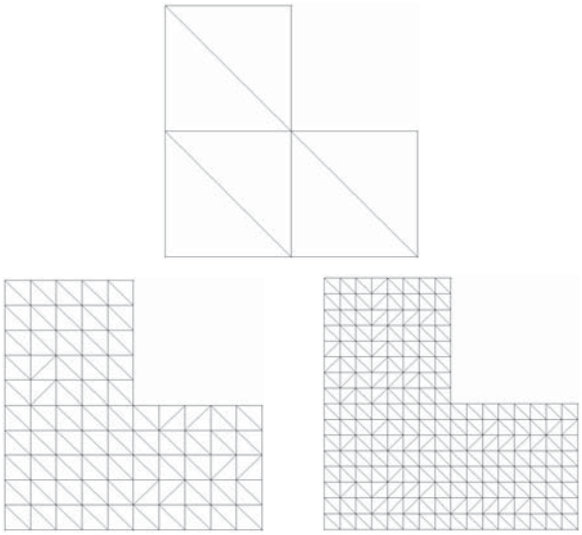

Figure 10. Uniform meshes in an L-shaped waveguide

The adaptation process has been tested for both refinement techniques (1:2 and 1:4). Figure 11 shows the adapted meshes throughout the process when a “longest edge” technique is applied, and figure 12 shows the results for the regular (maximum angle criterion) method. In both cases, the singularity is properly detected and the refinement is more intense in the singularity zone.

The convergence rate (figure 13) is similar for both cases, and much better than that obtained from a classical (uniform mesh) FEM. In fact, at the end of the process, the adaptation obtains a 10-times more accurate solution, for the same number of edges (about 600). In order to obtain this accuracy by means of a uniform mesh, it would be necessary about 10,000 edges.

Despite of the similar results in both refinement techniques, the 1:2 technique has needed 12 steps of refinement and, therefore, 12 FEM simulations, whilst the 1:4 refinement has obtained a similar error with 6 steps. So, the last refinement is preferable because it has a lower computational cost.

The improvement in the convergence rate is due to the progressive reduction and confinement of the error throughout the adaptation process. In figure 14, the distribution of the error density in the eigenvector (the electric field) for the meshes of the adaptive process (figure 12) is shown. Comparing these distributions with those obtained from the uniform meshes (figure 15) it is evident that the adaptation reduces the area with the highest error.

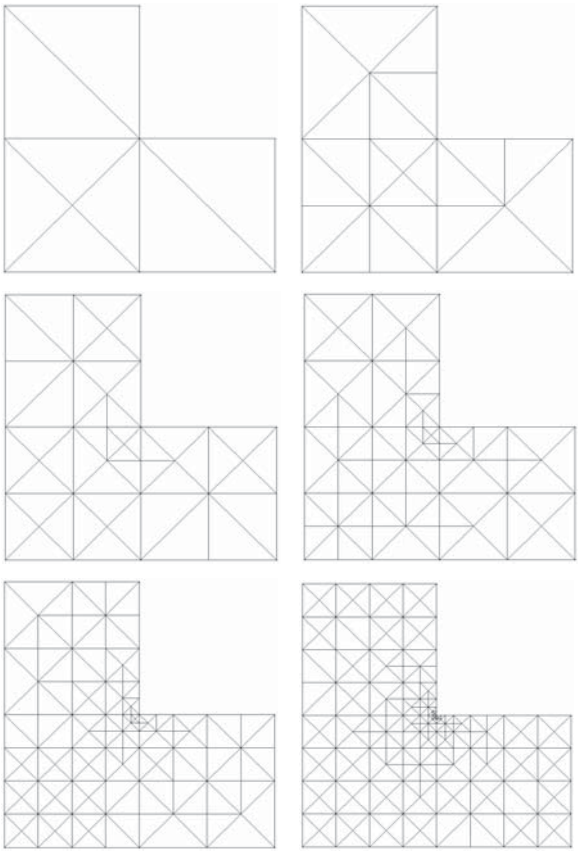

Figure 11. Adapted meshes (1st, 3rd, 5th, 7th, 9th and 12th) using 1:2 refinement

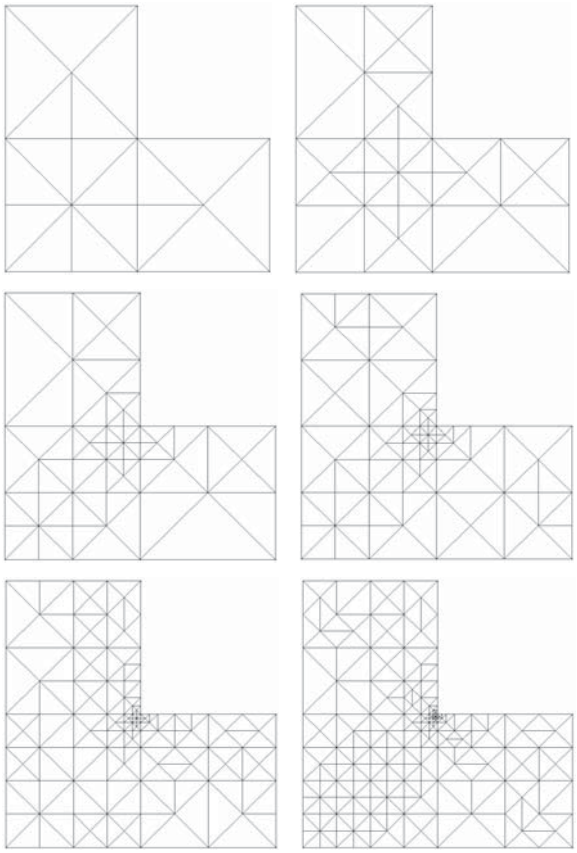

Figure 12. Adapted meshes (1st, 2nd, 3rd, 4th, 5th and 6th) using 1:4 refinement

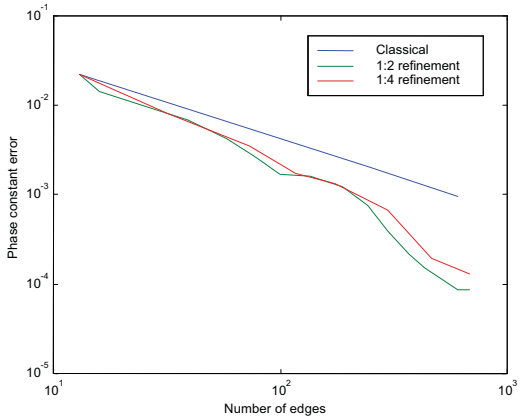

Figure 13. Convergence in the L-shaped waveguide

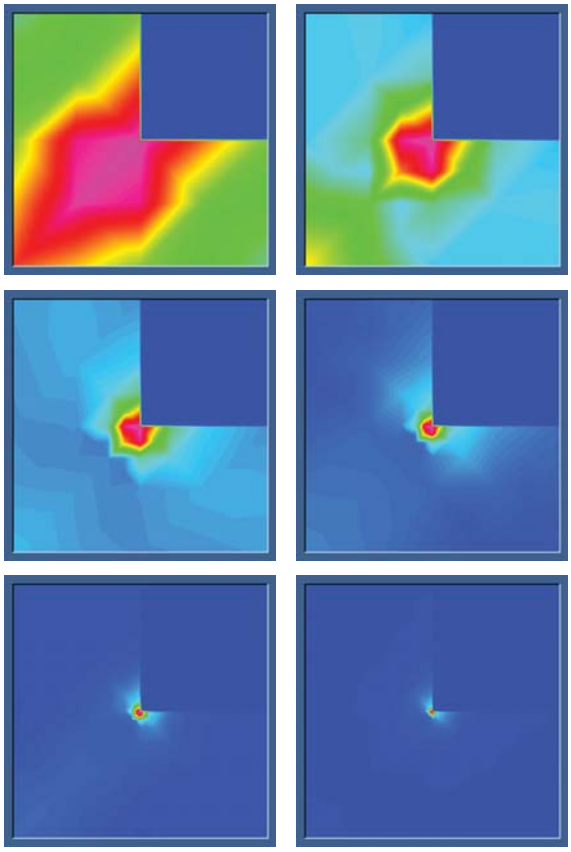

Figure 14. Distribution of the estimated error density in the adapted meshes

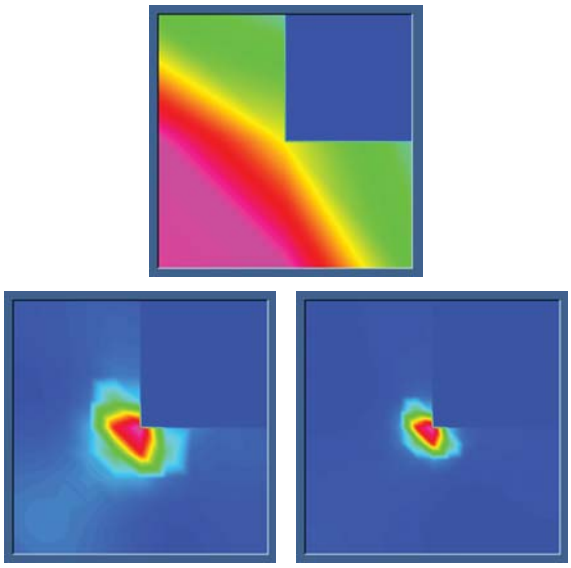

Figure 15. Distribution of the estimated error density in the uniform meshes

3.2. Shielded Microstrip Line

The structure shown in figure 16 consists of a substrate of a given relative electric permittivity (ε_{r2}), a metallic trip and a rectangular metallic framework.

In order to decrease the computational cost of the problem, the study of the adaptation has been carried out for one half of the whole domain, taking benefit from the symmetry of the waveguide. In this case, magnetic wall conditions are imposed in the plane of symmetry.

Comparing the refined meshes (figure 19) and the distribution of the transverse component (the dominant component) of electric field for the first mode (figure 17), it can be verified that refined regions are those where the electric field undergoes the biggest variation.

Figure 20 shows the convergence of the phase constant for the adaptation process compared with the convergence for consecutive graded meshes (figure 18). The convergence is clearly accelerated with the adaptive refinement.

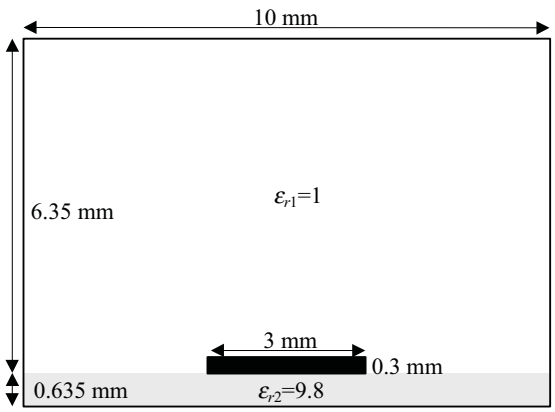

Figure 16. Cross-section of the microstrip line

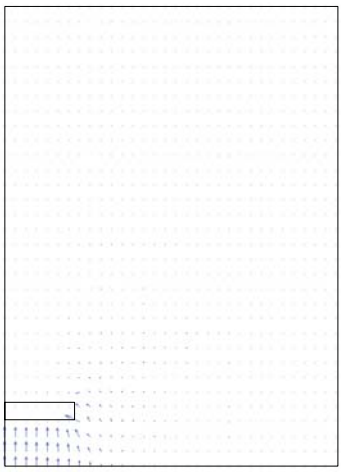

Figure 17. Transversal component of the first mode electric field in the microstrip line

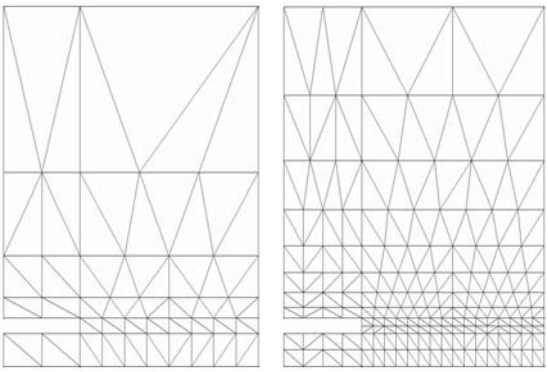

Figure 18. Graded meshes in the microstrip line

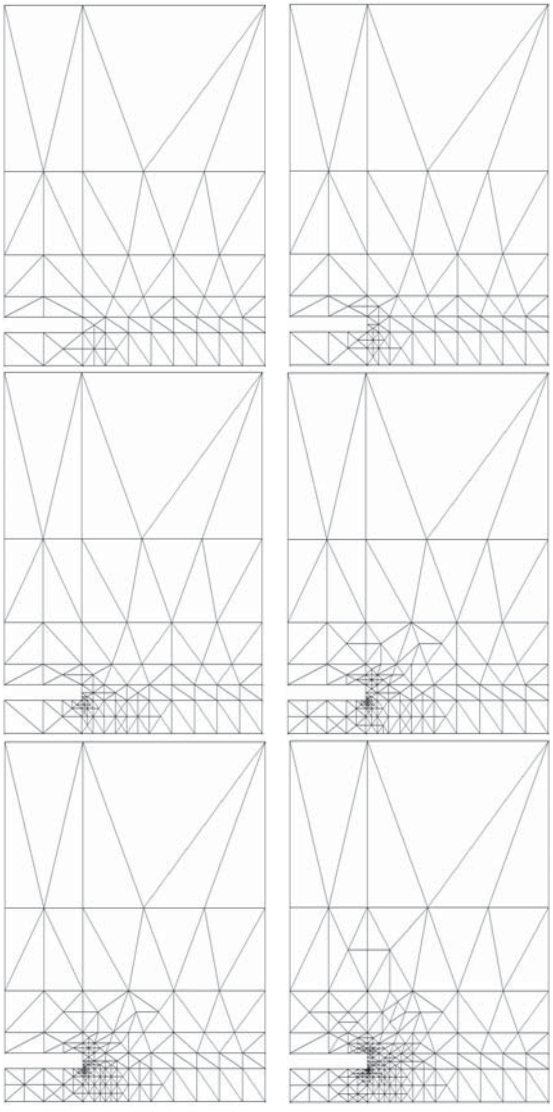

Figure 19. Adapted meshes (1st, 2nd, 3rd, 4th, 5th and 6th) using 1:4 refinement

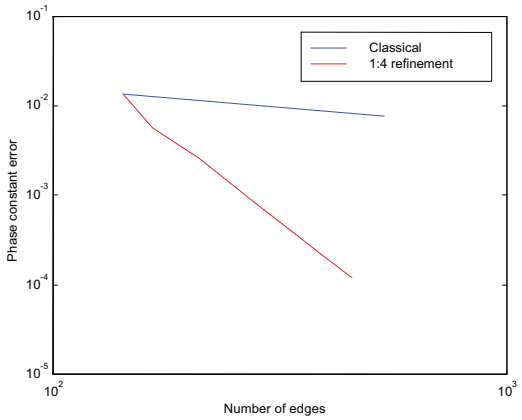

Figure 20. Convergence in the microstrip line

3.3. Shielded Unilateral Finline

Finally, a unilateral finline surrounded by a cylindrical metallic framework (figure 21) is analyzed. This structure consists of a substrate and a zero-thickness metallic strip. Again, this waveguide presents a symmetric cross-section. Therefore, only one half of the structure has been analyzed, imposing in this case an electric wall condition in the symmetry axis.

In the transversal component (the dominant one) of the first-mode electric field (figure 22) appears again a singularity, in this case near the edge of the strip.

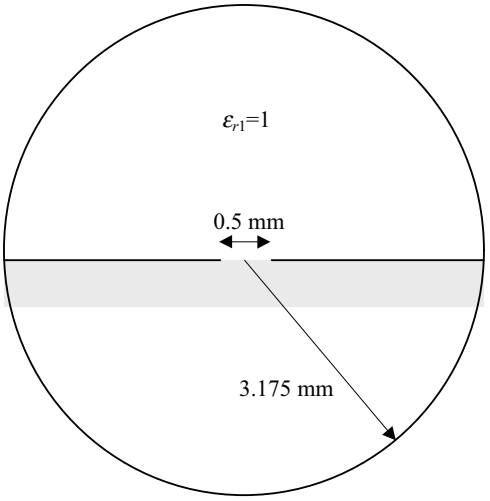

Figure 21. Cross-section of the unilateral finline

The meshes generated in the adaptation process (figure 24) indicate that, again, the singularity is properly detected and, therefore, the error in the problem is minimized with a little quantity of unknowns.

Figure 25 compares the convergence rate of the adaptive mesh refinement and that of the classical FEM (meshes of figure 23). At the end of the process, the adaptation obtains a 4-times more accurate solution, for the same number of edges (about 600). A similar accuracy can be obtained with a classical FEM and a graded mesh like those of figure 23, using about 40,000 edges. An HP C160 700 Series workstation needed about 8 hours for obtaining this accuracy by means of the adaptive procedure, whilst the use of 40,000 edges in a classical FEM will spend, due to the high computational cost of the eigensystem solving, about 50 years.

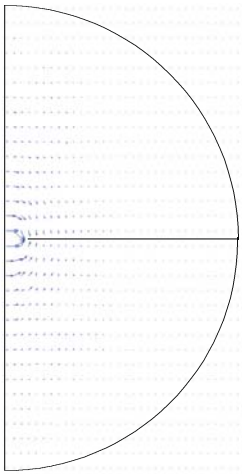

Figure 22. Transversal component of the first-mode electric field in the unilateral finline

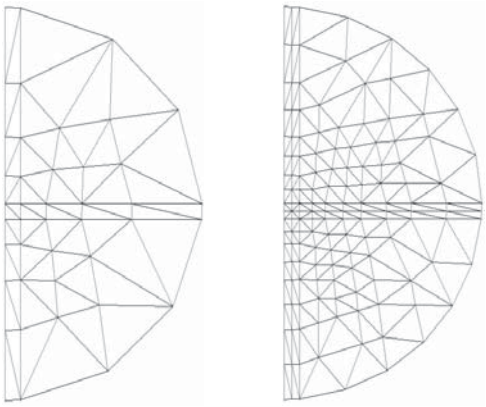

Figure 23. Graded meshes in the unilateral finline

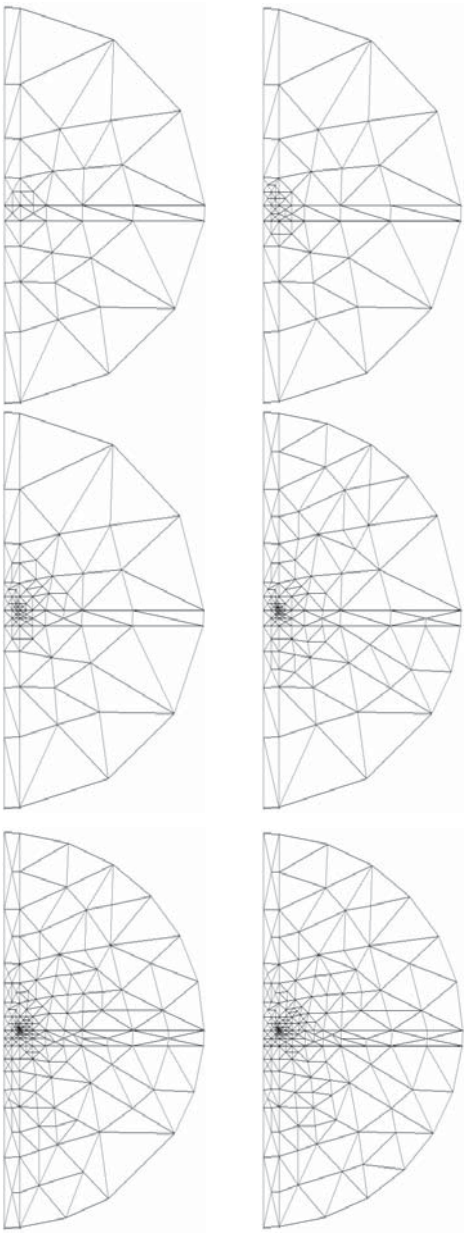

Figure 24. Adapted meshes (1st, 2nd, 3rd, 4th, 5th and 6th) using 1:4 refinement

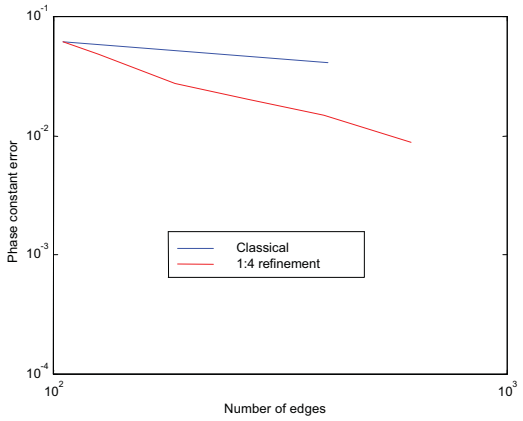

Figure 25. Convergence in the unilateral finline

4. CONCLUSIONS

The application of an adaptive mesh refinement procedure for solving the vector wave equation in transmission line electromagnetic problems has been presented. The indication of the elemental errors has been obtained by means of a residual error indicator. A one-level *h*-refinement, based on longest edge bisection and regular (maximum angle criterion) split, has been applied for the enrichment of the mesh.

After the element split, an element generation strategy has been performed for maintaining the conformity in the mesh and a bounded regularity of triangles along the adaptation process.

Results obtained with this procedure in several waveguiding structures show that the adaptive mesh refinement detects properly the regions of the problem where a bigger density of degrees of freedom is necessary. The intelligent distribution of the unknowns throughout the problem domain reduces the computational cost of the FEM application (time and memory resources) and allows more accurate solutions.

The next step in this research is the development of 3D error indicators for tetrahedra and the adequate refinement techniques in order to deal with problems in the design of cavities, circulators and other microwave devices.

REFERENCES

[1] D.W. Kelly, J.P.S.R. Gago, O.C. Zienkiewicz, I. Babuska, "*A Posteriori* Error Analysis and Adaptive Processes in the Finite Element Method: Part I - Error Analysis", *International Journal for Numerical Methods in Engineering*, Vol. 19, pp. 1593-1619 (1983)

[2] M. Salazar-Palma, T.K. Sarkar, L.E. García-Castillo, T. Roy, A. Djordjevic, *Iterative and Self-adaptive Finite Elements in Electromagnetic Modeling*, Artech House, (1998)

[3] O.C. Zienkiewicz, J.Z. Zhu, "The Superconvergent Patch Recovery and *a Posteriori* Error Estimates. Part 1: The Recovery Technique", *International Journal for Numerical Methods in Engineering*, Vol. 33, pp. 1331-1364 (1992)

[4] O.C. Zienkiewicz, J.Z. Zhu, "The Superconvergent Patch Recovery and *a Posteriori* Error Estimates. Part 2: Error Estimates and Adaptivity", *International Journal for Numerical Methods in Engineering*, Vol. 33, pp. 1365-1382 (1992)

[5] A. Díaz, L. Nuño, "A Simple Error Estimator for Adaptive Finite Element Analysis in Waveguiding Structures", *IEEE Antennas & Propagation Society. International Symposium 1999*, pp. 2634-2637 (1999)

[6] Z.J. Cendes, D.N. Shenton, "Adaptive Mesh Refinement in the Finite Element Computation of Magnetic Fields", *IEEE Transactions on Magnetics*, Vol. 21(5), pp. 1811-1816 (1985)

[7] P.L. Baehmann, M.S. Shephard, "Adaptive Multiple-Level *h*-Refinement in Automated Finite Element Analysis", *Engineering with Computers*, Vol. 5, pp. 235-247 (1989)

[8] P. Fernandes, P. Girdinio, M. Repetto, G. Secondo, "Refinement Strategies in Adaptive Meshing", *IEEE Transactions on Magnetics*, Vol. 28(2), pp. 1739-1742 (1992)

[9] P.L. George, *Automatic Mesh Generation. Application to Finite Element Methods*, John Wiley & Sons - Masson, (1991)

[10] R. Verfürth, *A Review of A Posteriori Error Estimation and Adaptive Mesh-Refinement Techniques*, Wiley-Teubner, (1996)

[11] A. Díaz, L. Nuño, "Meshing of Arbitrary 2D-geometries in the Finite Element Method by Means of an Advancing Front / Interpolation Combined Technique", *Computational Mechanics. New Trends and Applications (Proceedings on the Fourth World Congress on Computational Mechanics)* (1998)

[12] A. Díaz, L. Nuño, "Grid Generation of Arbitrary 2D-Geometries by Means of an Advancing Front / Interpolation Hybrid Technique", *Numerical Grid Generation in Computational Field Simulations (Proceedings of the Sixth International Conference)*, pp. 403-410 (1998)